

## Supplementary Material

# Enhanced photoelectrochemical response of SnSe<sub>2</sub> nanosheets

Zhen Fang,<sup>\*a</sup> Shenghua Hao,<sup>a</sup> Liuyang Long,<sup>a</sup> Hui Fang,<sup>a</sup> Tingting Qiang<sup>a</sup>  
and Yixuan Song<sup>a</sup>

<sup>a</sup> Key Laboratory of Functional Molecular Solids, Ministry of Education.  
Center for Nano Science and Technology. College of Chemistry and  
Materials Science, Anhui Normal University, Wuhu, 241000, P. R. China;  
E-mail: fzfsen@mail.ahnu.edu.cn

### S1. Experimental section

#### 1.1 Preparation of stacked SnSe<sub>2</sub> nanosheets

All the chemicals were of analytical grade and used as received without further purification. In a typical synthesis of SnSe<sub>2</sub> nanosheets (SnSe<sub>2</sub> NSs), SnCl<sub>2</sub>·2H<sub>2</sub>O (0.1 mmol), SeO<sub>2</sub> (0.1 mmol), and poly (vinyl pyrrolidone) (PVP, 6 g) is added into benzyl alcohol (40 mL). After vigorous magnetic stirring at room temperature for 0.5 h, a deep orange-colored suspending solution was formed. Then the mixture was transferred into a 60 mL teflonlined stainless steel autoclave and heated at 180 °C for 16 h. The product was obtained by centrifuged at 8000 rpm for 5 minutes. After washed several times with absolute alcohol and acetone, the product was dried at 80 °C in air. To study the influence factors on the composition, size, and shape of the final product, the experimental parameters, such as the surfactant and the solvent, have been varied during the synthesis of SnSe<sub>2</sub> NSs.

#### 1.2 Preparation of SnSe<sub>2</sub> nanoplates

In a typical synthesis of  $\text{SnSe}_2$  nanoplates ( $\text{SnSe}_2$  NSs), when the experiment was take place at 220 °C with other reaction conditions remain the same as the synthesis of  $\text{SnSe}_2$  nanosheets,  $\text{SnSe}_2$  nanoplates (NPs) was got.

	synthesis temperature	diameter	thickness
$\text{SnSe}_2$ NSs	180 °C	~1 $\mu\text{m}$	~20 nm
$\text{SnSe}_2$ NPs	220 °C	~5 $\mu\text{m}$	~200 nm

Table 1

### 1.3 Sample characterization

The resulting products were characterized with X-ray powder diffraction (XRD) using a Shimadzu X-ray diffractometer (XRD-6000) with Cu K $\alpha$  irradiation ( $\lambda = 1.54187 \text{ \AA}$ ). The morphology of the as-prepared samples was examined by field-emission scanning electron microscopy (FESEM, Hitachi S-4800 at an accelerating voltage of 5 kV). High-resolution transmission electron microscopy (HRTEM) images, selected area electron diffraction (SAED) were obtained from a FEI tecnai G2 transmission electron microscope working at an accelerating voltage of 200 kV. Before HRTEM observation, the sample was dispersed in alcohol through an ultrasonication process, and then a drop of the dispersion was placed on a copper grid coated with carbon film, which was dried naturally at room temperature. UV-vis-NIR diffuse reflection spectra of the supernatants were collected on a DUV-3700 UV-vis-NIR spectrophotometer at room temperature. The electronic structure of the product was characterized with X-ray photoemission spectroscopy (XPS, Kratos Axis UltraDLD, monochromatized Al K $\alpha$  source) operated at a base pressure of  $5 \times 10^{-10}$  Torr. Atomic force microscopy (AFM) measurements were conducted with a Mutilmode V AFM system (Veeco).

Liquid Chromatography-Mass Spectrometry (LC-MS MOF Agilent 6200) was used to analyze the solvent after reaction.

#### 1.4 Potoelectrochemical measurements

The Potoelectrochemical (PEC) tests were carried out in a conventional three-electrode. A Pt mesh and Ag/AgCl were used as the counter and reference electrodes, respectively. In a typical preparation of working electrode, 0.02g SnSe<sub>2</sub> NSs or 0.02g SnSe<sub>2</sub> NPs were dissolved in 1mL absolute alcohol, then 0.3 mL of the prepared solution were deposited on the ITO substrate employed as the working electrode with an area of 2\*2 cm<sup>2</sup>. 0.1 M Na<sub>2</sub>SO<sub>4</sub> solution was used as the electrolyte (pH=7.5). Current – voltage curves, impedance – potential measurements were recorded by an electrochmical workstation (CHI 660D, Chenhua Co., Ltd., China). A 500 W Xe lamp (CHF-XM-500, Changtuo Technology Co., Ltd.) equipped with an ultraviolet cutoff filter ( $\lambda > 400$  nm) were employed to study visible light-dependent PEC response. The integrated visible light intensity was calculated. 200 mW · cm<sup>-2</sup> measured with a radiometer.

#### S2. XRD pattern obtained by drop-casting the products dispersed in anhydrous ethanol onto planar substrates

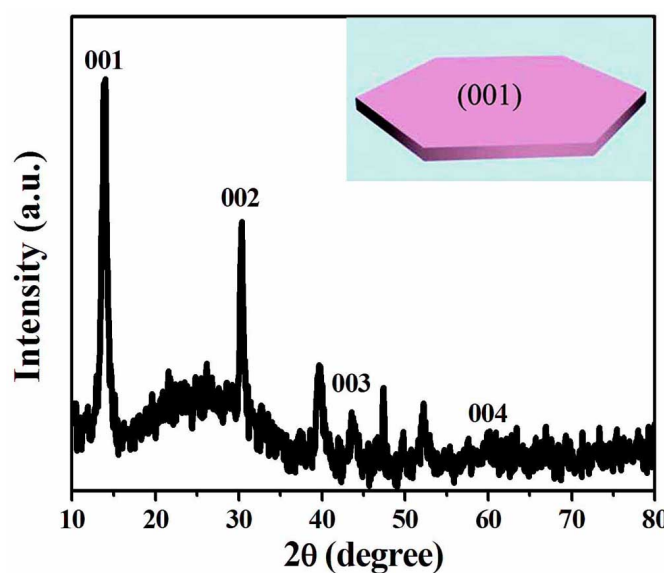


**Fig. S1.** (001)-oriented XRD pattern of SnSe<sub>2</sub> nanosheets.

### S3. XPS spectra of SnSe<sub>2</sub> nanosheets

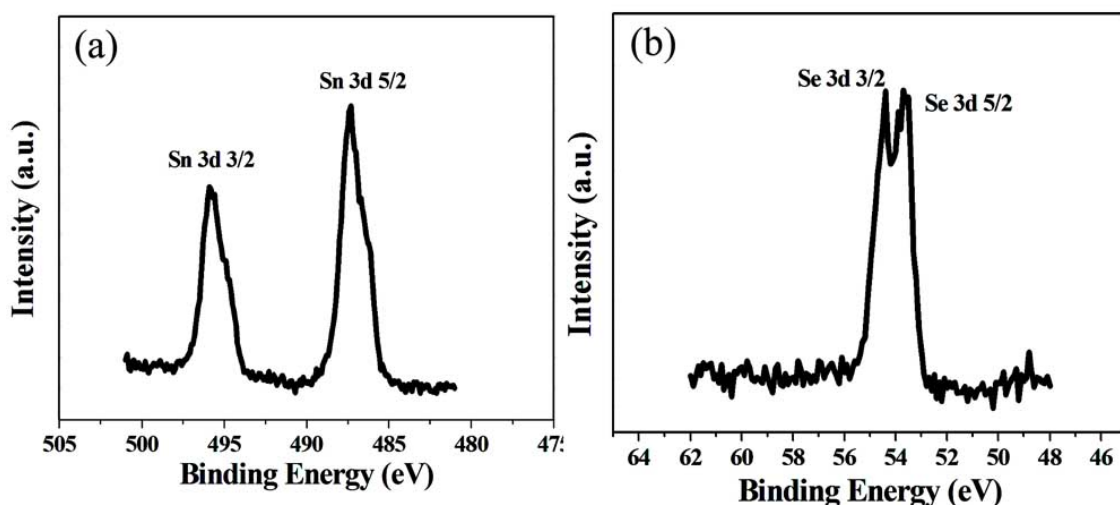


**Fig. S2.** X-ray photoelectron spectroscopy of the products.

### S4. Crystal structure of hexagonal SnSe<sub>2</sub> and AFM of SnSe<sub>2</sub> nanosheets

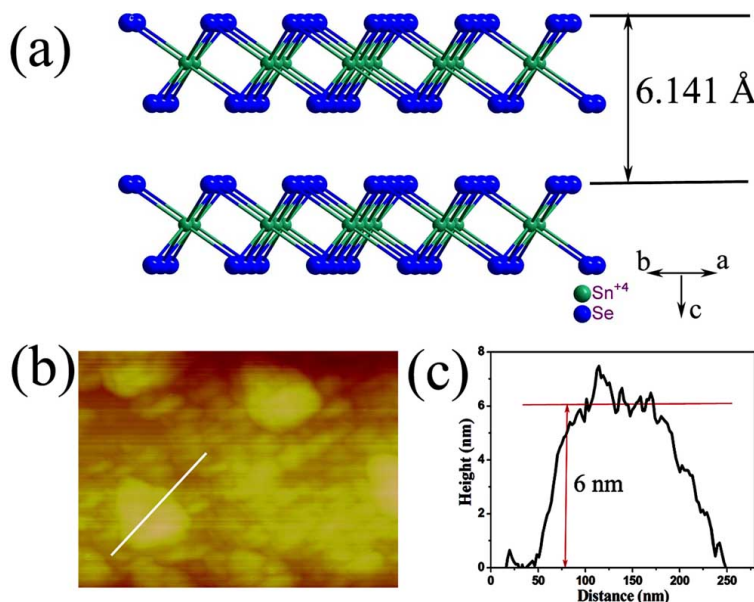


**Fig. S3.** (a) The schematic unit cell structure of hexagonal SnSe<sub>2</sub>, in which the triple layer of Se-Sn-Se is separated by 6.141 Å. (b) AFM image and (c) The corresponding height profile of SnSe<sub>2</sub> NS.

### S5. Effects of the solvent

In our experiment, benzyl alcohol reduced Se to Se<sup>2-</sup>. If ethanol or water

with less reducibility were used as solvent instead of benzyl alcohol, only hexagonal structural selenium was obtained (Fig. S4). The results show that benzyl alcohol is an appropriate solvent that is helpful to get the phase pure  $\text{SnSe}_2$ .

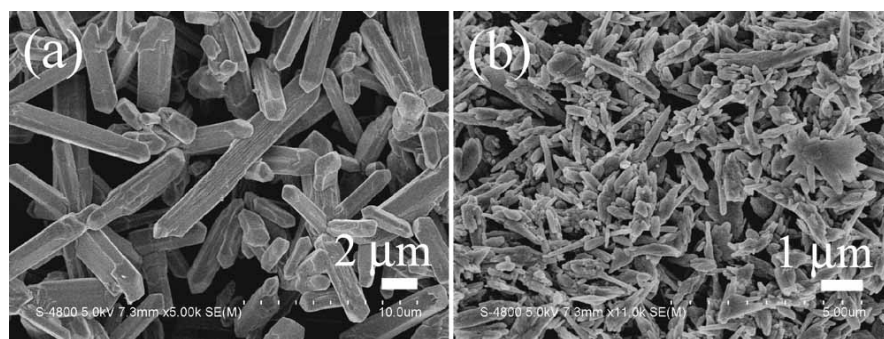


**Fig. S4.** SEM images of Se precursor when (a) Using ethanol as reation solvent. (b) Using water as reaction solvent.

## S6. Effect of temperature

The experimental temperature also has effect on the final product. XRD and SEM results (Fig. S5) showed that only hexagonal structural Se was obtained at low temperature ( $160\text{ }^\circ\text{C}$ ). Thicker  $\text{SnSe}_2$  nanoplates (NPs) were got at higher temperature ( $220\text{ }^\circ\text{C}$ ). As shown in Fig. 1f, the  $\text{SnSe}_2$  NPs are  $\sim 200\text{ nm}$  thickness and  $5\text{ }\mu\text{m}$  in diameter. It indicated that  $180\text{ }^\circ\text{C}$  is the most appropriate temperature to synthesis  $\text{SnSe}_2$  nanosheets.

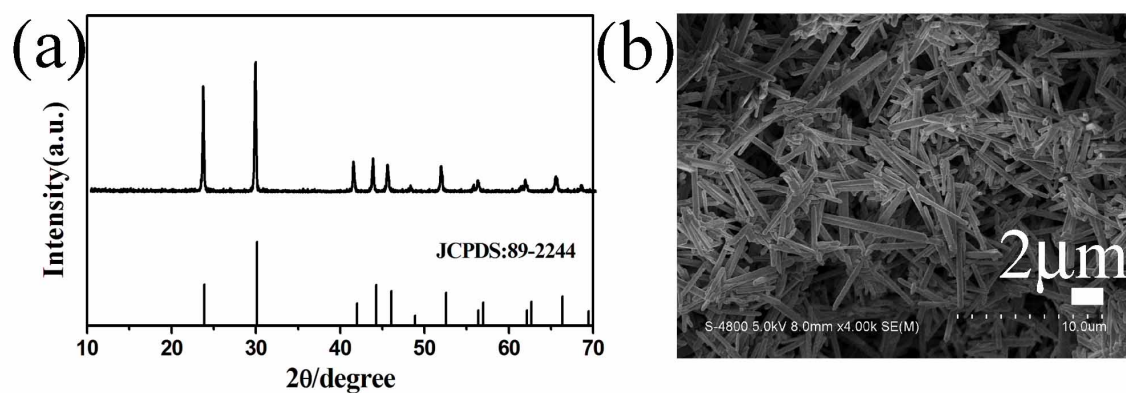


**Fig. S5.** (a) XRD pattern of Se obtained at  $160\text{ }^\circ\text{C}$  and (b) SEM image of Se obtained at  $160\text{ }^\circ\text{C}$ .

**S7. SEM image of as-synthesized samples obtained by using 8 g PVP**

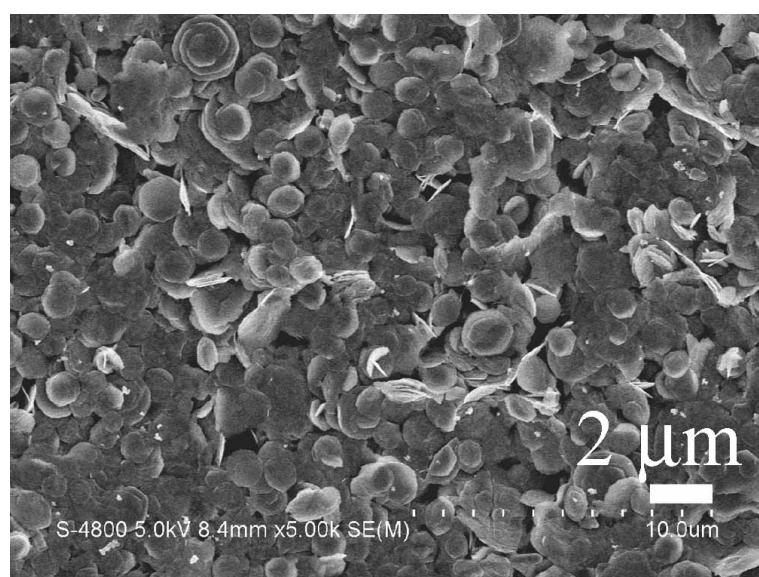


**Fig. S6.** SEM image of as-synthesized samples obtained by using 8g PVP

**S8. Digital images of as-synthesized samples obtained by using different surfactant at the room temperature.**



**Fig. S7.** (a) The instantaneous digital image of adding different surfactants. (b) The digital image of adding different surfactants after 3 hours at room temperature. The second breakers are the reaction reagents with no surfactant.

**S9. SEM images of as-synthesized samples obtained by using different surfactant.**

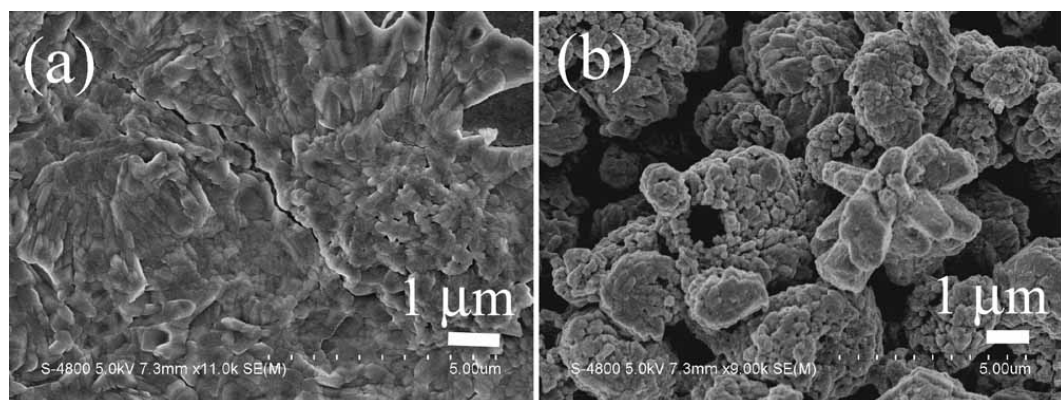


**Fig. S8.** (a) SEM image of using CTAB as surfactant. (b) SEM image of using PAA as surfactant.

**S10. Digital image of the Sn (IV) complex solution**

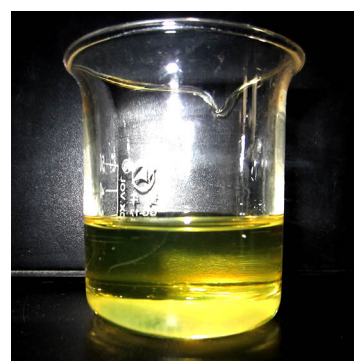


**Fig. S9.** Digital image of the solution obtained when  $\text{SnCl}_4 \cdot 5\text{H}_2\text{O}$  and PVP was solvothermal treated in benzyl alcohol

### S11. XRD of different reaction stages

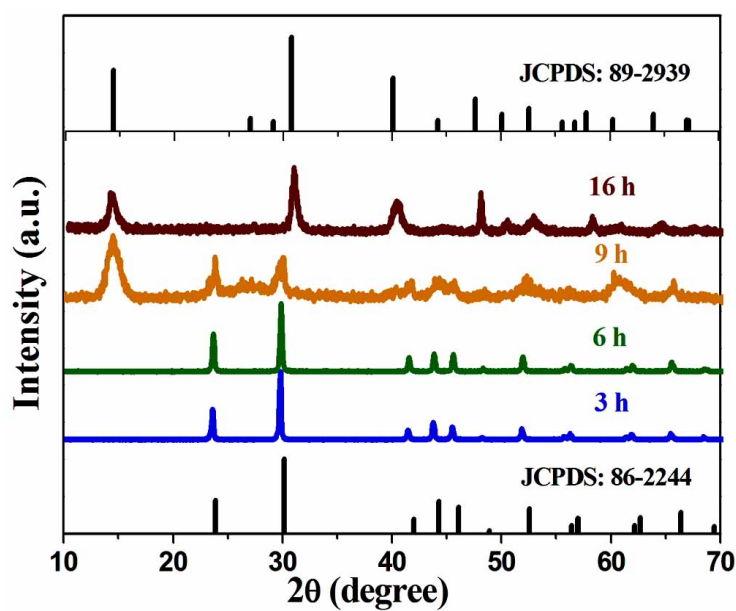


**Fig. S10.** XRD images of as-synthesized samples obtained by hydrothermal reaction for different time.

### S12. SEM images of different reaction stages

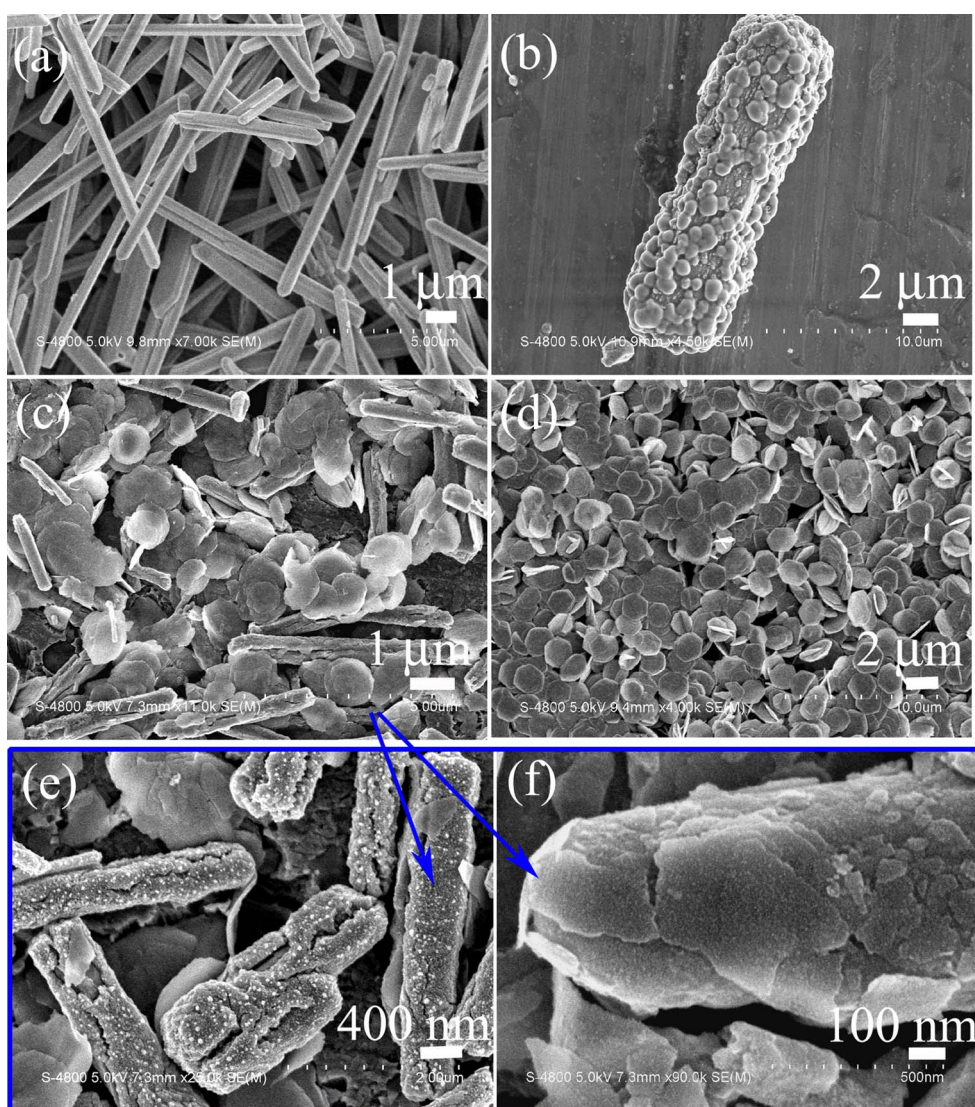


**Figure S11.** SEM images of aliquots taken from the different reaction stages. (a) 3 h, hexagonal structural Se. (b) 6 h, SnSe<sub>2</sub> nanoparticles were formed on the surface of rod-like Se. (c) 9 h, irregular SnSe<sub>2</sub> thinner sheets were fabricated. (d) 16 h, perfect SnSe<sub>2</sub> nanosheets. (e) and (f) the high magnification SEM images of (c).

**S13. LC-MS of The obtained solution after reaction for 6 h**

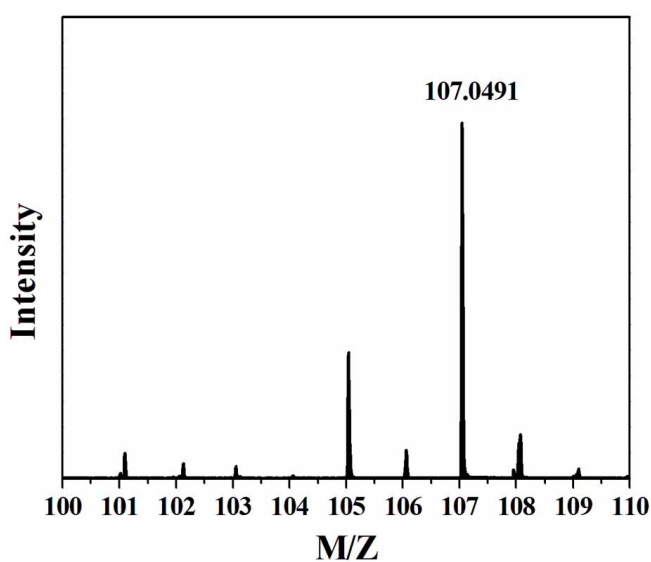


**Figure S12.** Mass spectra of the benzaldehyde.

**S14. Indirect and direct band gaps of the SnSe<sub>2</sub> NSs and SnSe<sub>2</sub> NPs**

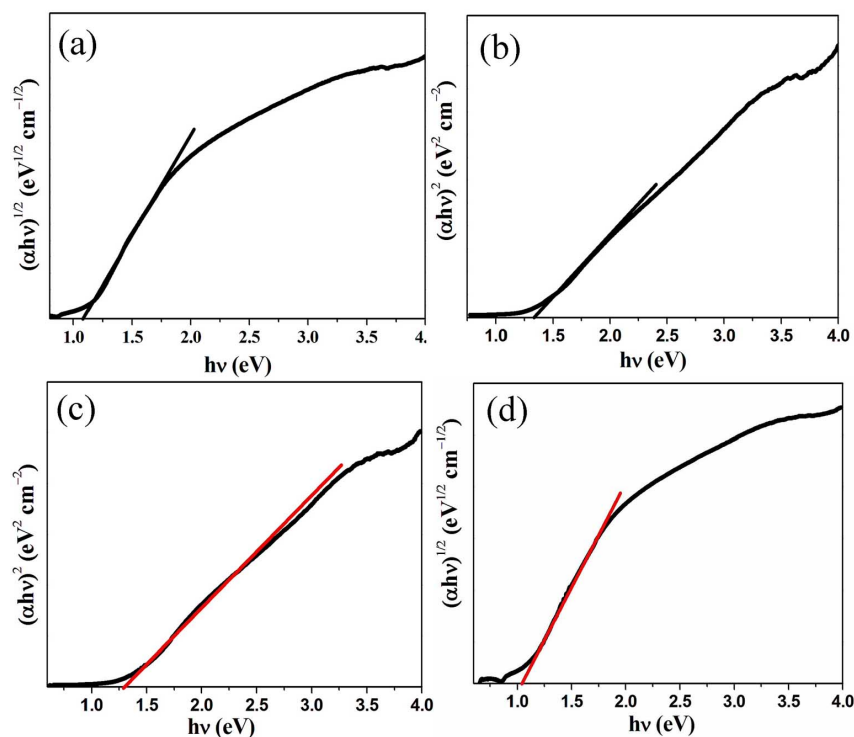


**Fig. S13.** (a) Direct band gap and (b) Indirect band gap of the SnSe<sub>2</sub> NSs.  
(c) Direct band gap and (d) Indirect band gap of the SnSe<sub>2</sub> NPs.

### S15. Characterization of the samples dropped on the ITO substrate

Fig. S14 showed the SEM images of ITO substrate with the prepared samples. Fig. S14a, b, c are the images of three segments of ITO substrate with  $\text{SnSe}_2$  NSs, it showed that the thickness of the  $\text{SnSe}_2$  NSs deposited on the ITO substrate was about 3-3.5  $\mu\text{m}$ . Fig. S14d, e, f are the images of three segments of ITO substrate with  $\text{SnSe}_2$  NPs, it showed that the thickness of the  $\text{SnSe}_2$  NSs deposited on the ITO substrate was about 4-5  $\mu\text{m}$ . It obvious that the stacking density of the  $\text{SnSe}_2$  NSs samples are much bigger than  $\text{SnSe}_2$  NPs, thus the thickness of the  $\text{SnSe}_2$  NSs deposited on the ITO substrate was smaller than the thickness of the  $\text{SnSe}_2$  NPs.

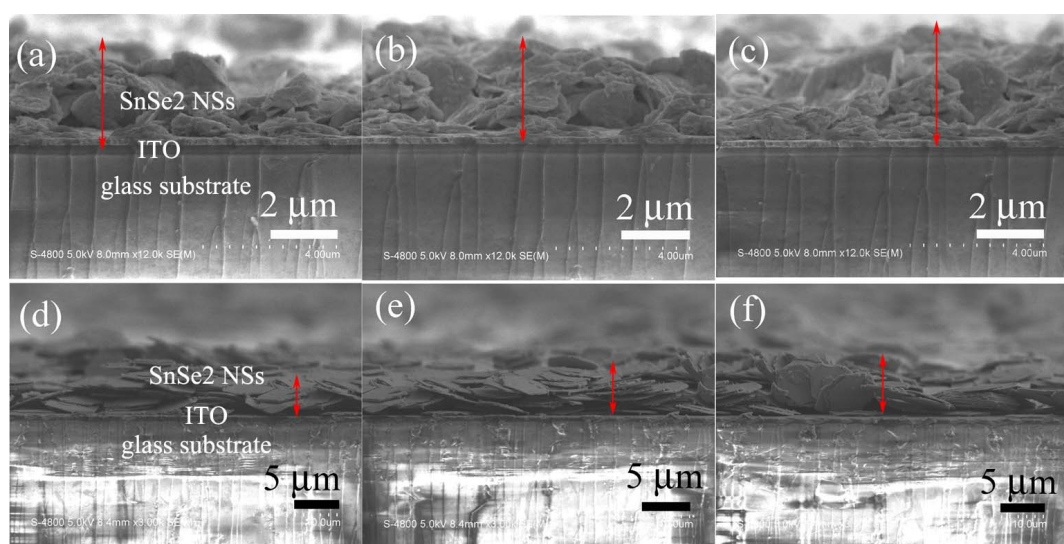


**Fig. S14.** (a-c) the SEM images of three segments of ITO substrate with  $\text{SnSe}_2$  NSs. (d-f) the SEM images of three segments of ITO substrate with  $\text{SnSe}_2$  NPs.